JOURNAL OF MATERIALS SCIENCE 29 (1994) 1701–1706

The role of silicon-particle defect structure during low-temperature nitriding

T. S. BARTNITSKAYA, M. V. VLASOVA, N. G. KAKAZEI, T. V. TOMILA
The Institute for Materials Science Problems, Ukrainian Academy of Sciences, Krzhyzhanovsky St, 3, Kiev, Ukraine

The nitriding of silicon powders of different particle size, produced by jet and ball milling, is considered. The nitride formation is found to be affected by the defect density of the silicon particles' surface layers. The volume nitriding of silicon powders was determined by a chemico-mechanical effect consisting of surface-microcrack opening.

1. Introduction

In recent years, research efforts have focused on the mechanisms of silicon-nitride formation in the reaction: $3Si + 2N_2 \rightarrow Si_3N_4$ [1–3]. Thus, a detailed analysis was made of the effect of different heat treatment regimes [1, 4], of the impurity nature and the effect both in silicon and the nitride [5, 6] of silicon particle sizes [7, 8], etc. However, the relationship between silicon-particle structure states and their nitriding has not yet been studied, although the effect of a silicon-nitride preliminary treatment was noted in [8].

The present research was intended to partially fill this gap and to consider the effect of the defect states formed by preliminary mechanical treatment of silicon powders on their subsequent nitriding.

According to [9, 10], the particle defect structure of covalent compounds having diamond-like lattices after crystal comminuting is spatially inhomogeneous. The particles are supposed to consist of weakly deformed cores surrounded by a highly defective layer with numerous microcracks. The microcracks determine the structure of the coherent scattering regions (CSRs). There are also amorphous-material interlayers, localized on their boundaries. The average surface-layer thickness in the particles produced under similar conditions is insignificantly dependent on their size, d, at least for $d > 1$ μm.

As is shown in [11], mechanical treatment of silicon crystalline powders using different powder dispensers results both in their comminution and in aggregates forming from the particles. Depending on the dispenser type, the powder may contain certain impurities, and, in the case of treatment in air, oxidized silicon. The results of fine-silicon-powder nitriding are interpreted in terms of the concept of their defect structure, presented above.

2. Experimental procedure

The samples for nitriding were produced by comminuting silicon crystalline powders with an average particle size of about 35 μm in a jet mill and activator (see Table I). A dispersion analysis was carried out using an SK laser micrometre sizer PRC-700 and a micrometre photo-sizer SKC-2000. The specific area of the surface was determined by a Brunave–Emmett–Teller method (BET). To control the effects of the surface defect states induced by mechanical treatment, a series of silicon powders were etched with fluorhydric acid. Some experiments were also carried out to eliminate iron impurities in the samples. These samples were treated with 50% HCl.

Silicon powders were nitrided in a nitrogen flow at a nitriding temperature of $T_N = 1473$–1673 K. The nitriding time, t_N was varied from minutes up to some hours. The nitrogen content in the samples, C_N, was determined according to a standard procedure. To eliminate surface-oxide complexes, chloric ammonium was added to silicon powder.

TABLE I Comminution conditions and the particle size of silicon powders

Sample Number[a]	Regime and preparation technique	d (μm) laser	d (μm) sedimentation	Fe (mass %)
1	Starting	35		0.01
	Activator-comminutor			
	Hardmetal balls			
	Comminution in alcohol			
	Comminution time (min)			
5	5	3.7	0.41	0.42
6	8		0.35	0.48
7	Centrifuging at 2500 rev min^{-1}	0.8	0.3	0.46
	Comminution in a jet mill in air			
10	(a) $P = 6$ atm (b) $P = 7.5$ atm	2.4	0.72	0.1
11	Sampling from cyclone	2.1	0.7	0.13
12	sampling from filter	0.6	0.19	0.09

[a]The sample numbers correspond to the designations in [11].

0022–2461

Both the starting silicon samples and their nitriding products were studied using an X-ray diffractometer, HZG-4A, a radio-spectrometer, SE/x 2547 (3 cm band), at room temperature, an infrared (I.R.) spectrometer, Specord M80, and two transmission electron microscopes, HU-200F and JEM-100CX.

3. Experimental results

3.1. Dispersion measurements

Fig. 1a shows the specific surface area, S_{sp}, of silicon powders as a function of the I/d_{av}-value. For the system of single particles, this dependence is linear. Deviation from linearity for the samples with $S_{sp} > 8$–$10\ m^2\ g^{-1}$ indicates that particles have aggregated. Chemical etching of such powders in HCl for 20 min did not appreciably change the value of S_{sp}, however, it facilitated reduction in d_{av}, that is aggregate fracture.

3.2. Nitriding method

In a stoichiometric sample, the Si_3N_4 nitrogen content is 39.6 wt %. The data on nitriding kinetics for different samples at 1473 K (Figs 1 and 2a) show nitriding to be more effective in the initial stages for larger values of S_{sp}. The nitriding degree increases with increases in the temperature of treatment (Fig. 2b).

Since nitriding at 1473 K for 1 h mainly involves surface states, one should expect a proportional dependence between C_N and S_{sp}. However, as follows from Fig. 1, the character of the change in $C_N(S_{sp})$ is qualitatively similar to that of $I/d_{av}(S_{sp})$. This makes it possible to establish a relationship between the nitriding of silicon powders, with $S_{sp} > 8\ m^2\ g^{-1}$, and average-sized aggregates contained in them.

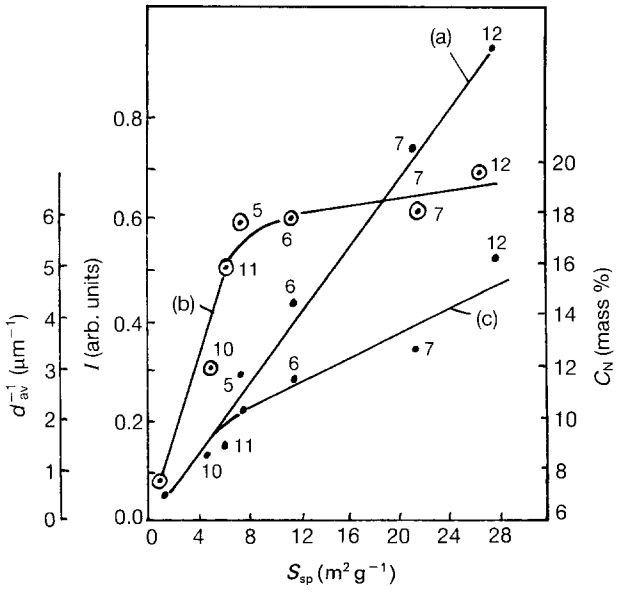

Figure 1 (a) The EPR signal intensity, (b) the reverse value of the silicon particles average size, and (c) the nitrogen content after silicon-powder nitriding as functions of the Si powders' specific surface area. For (c), $T_N = 1473$ K and $t_N = 1$ h. The numbered points correspond to the different techniques and regimes of comminution in Table I.

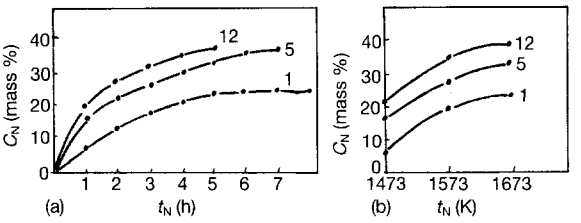

Figure 2 The nitrogen content in silicon powder as a function of (a) the nitriding time ($T_N = 1473$ K), and (b) the nitriding temperature ($t_N = 1$ h). The numbered curves correspond to the sample numbers in Table I.

It should be noted that no appreciable nitriding of the silicon powders with etched surface layers occurs in the given temperature range (especially at 1473 K). This is a direct indication of the responsibility of the silicon-particle surface-defect states for the-low temperature nitriding. In turn, the practically complete nitriding of the unetched samples with $d < 3$ μm at $T_N \geqslant 1473$ K and $t_N > 4$ h indicates the responsibility of the surface-defect layer for the volume silicon-powder nitriding as well.

3.3. X-ray studies

The principal parameters to be determined in the silicon phase were the CSR size, D, and the magnitude of microdistortions, $(\Delta a/a)$, which were evaluated from widening of the X-ray lines (4 4 0) and (2 2 0) according to the standard procedure [12]. These parameters characterized the general level of the sample defect density. Fig. 3 shows the variation in D and $\Delta a/a$ as a function of the nitriding time for different silicon powders. Note the reduction in the microdistortion dimension and the increase in CSR after 1 h of nitriding. At $t_N > 1$ h, for sample number 1 ($d \sim 35$ μm), $\Delta a/a$ increases and D decreases. This indicates the emergence of a new source of stress in silicon particles during nitriding. In finer powders, due to a sharp decrease in the silicon content with t_N growth, the initial stages of nitriding can be traced only when t_N is small.

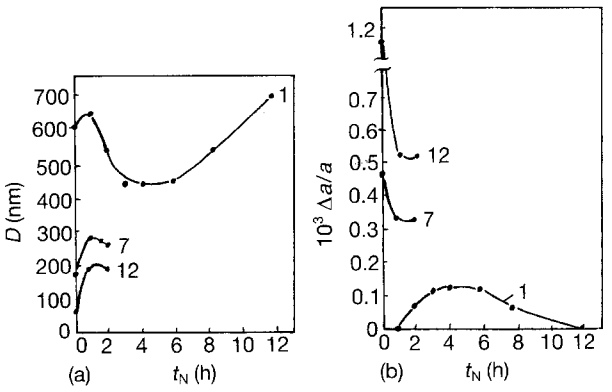

Figure 3 (a) The CSR size and (b) the microstress magnitude in the silicon phase as a function of Si-powder nitriding time. $T_N = 1473$ K. The numbered curves correspond to the sample numbers in Table I.

Using X-ray analysis, the ratio of the α- and β-phases in Si_3N_4 after nitriding was evaluated. In the temperature range under consideration, the main crystalline phase was α-Si_3N_4. With the increase in t_N and T_N, the β-phase content increased, however, it did not exceed 10%.

3.4. Electron paramagnetic resonance (EPR) data

In silicon samples, after they have been cleaned from magnetic impurities, a typical for the comminuted silicon EPR signal, with $g = 2.0055 \pm 0.0002$ and with a width of about 5.5×10^{-4} T, is registered. Such a signal is considered to be due to the formation of amorphous-silicon interlayers on CSR boundaries in the surface-distorted layers of particles [10]. The EPR signal amplitude, I, is proportional to the silicon powders' specific surface area (including initial one) (Fig. 1, curve (a)) which makes it possible to speak, essentially, of the same type of surface layers structures as are formed during mechanical treatment. In the samples etched in fluorhydric acid, such a signal was not observed; this is due to removal of the highly defective surface layer.

Disappearance of the EPR signal during the initial nitriding period (Fig. 4) reflected annealing of paramagnetic centres. Such a change agrees with the data presented in [13]. The authors of [13] show that, during heat treatment of the comminuted silicon crystals for 10 min in air at about 673 K, approximately 80% of paramagnetic centres are annealed, the rest are completely eliminated at 1073 K. Paramagnetic-centre annealing is one of the stages of the amorphous-silicon-interlayer crystallization.

3.5. Electron microscopy data

After mechanical treatment, silicon powders are single crystalline particles with traces of both brittle fracture and plastic deformation. There is a tendency for particle agglomeration with decreases in particle size.

In the samples produced by the starting silicon-powder ($d_{av} \sim 35\mu m$) nitriding at 1473 K, a nitride layer with a grain structure was observed on the particle surface. In finer powders (for example, number 12), there are silicon particles not covered with a nitride layer. α-Si_3N_4 fibres were mainly found in the finer powder at the initial stage of nitriding. In the samples produced at $T_N \geqslant 1473$ K and $t_N > 1$ h, nitrides are present both as fibres and particles with $d \sim 1$ μm, as single-crystalline elongated plates or as polycrystals with an obvious grain cut. An elongated particle form is predominant.

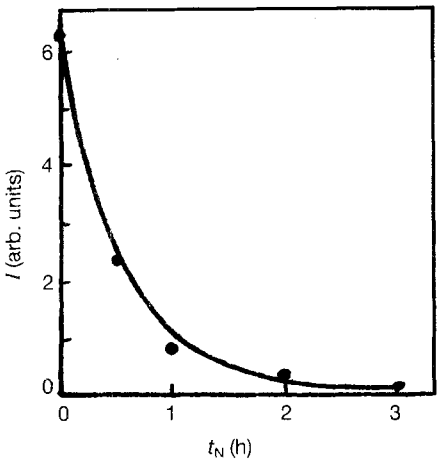

Figure 4 The change of the EPR-signal amplitude in silicon during nitriding of sample number 12. $T_N = 1473$ K.

3.6. I.r.-spectroscopy data

In silicon powders produced by comminution in air, or after their durable storage, absorption bands are observed, they are related to the sorbed oxygen and (or) an oxide form of a SiO_x-type [14] (Table II). Nitriding at $T \sim 973$ K results in an increase in the band intensities corresponding to the Si–N and the Si–O bonds. The latter reflects silicon-powder oxidation with the oxygen present in nitrogen. At $T_N \sim 1473$ K, with the increase in nitriding time, the processes may be singled out as follows: partial silicon oxidation → reduction in oxide content and formation of amorphous silicon nitride → reduction in amorphous-silicon-nitride content and formation of α-Si_3N_4. In the samples produced at higher T_N and t_N-values, weaker bands are registered as characteristic for β-Si_3N_4 (see Table II).

4. Discussion

An intricate character of the defect structure of the starting silicon samples (involving surface defect layers, microcracks, volumetric stress, amorphous interlayers, a wide particle-size distribution, availability of aggregates of different geometries, and inclusion of impurities of oxides) supposes ambiguity and multiplicity of the nitriding process. Evolution of the spatial inhomogeneous defect structure during nitriding involves a variety of competitive and supplementary processes. Thus, initial heating, on the one hand, facilitates annealing of the silicon-particle defect structure induced by the preliminary treatment; and, on the other hand, it promotes participation of high reactivity of the surface-defect layers. The former results in the weakening of intrinsic stresses in silicon particles, and the latter initiates nitriding, acidification and volume diffusion of gases in microcrack passages. Thus, in the surface layers, new phases ($(Si_3N_4)_{am}$ and SiO_x) are formed and microcrack curing is hindered.

The data obtained make it possible to plot a chart of the structure and phase changes taking place in the Si–N system (Fig. 5). As can be seen, fibre formation during the initial treatment correlates with the appearance of SiO_x in the system (where $x \approx 2$) and of $(Si_3N_4)_{am}$. This may be related both to the relatively low melting point of the former [15] and to the diffusion activity of the latter. It is quite possible that both the phases formed, and the amorphous surface layers, take part in the primary aggregate densification and agglomerate formation from silicon particles. As a result, nitriding is somewhat hindered, and the nitrogen content, C_N, is found to be proportional to I/d_{av}.

TABLE II The Characteristics of i.r. absorption bands in silicon powders after nitriding

Sample number	T_N (K)	t_N, (min)	Frequency of i.r. absorption, ν (cm^{-1})															Phase composition
			1	2	3	4	5	6	7	8	9	10	11	12	13	14	15	16	
1	initial				515_{w*}		600_{w*}								1106_{w*}			1220_{w}	Si*, $SiO_x(x<2)$
	1473	5	462_{w}	494^{wd}_{w}								900^{wd}_{w}			1100^{av}_{wd}		1165_{av}	1225^{av}_{wd}	Si*, $SiO_x(x<2)$, Si_3N_4 am
		30	400^{av}_{n} 445_{w}	480_{av} 500_{sh}	520_{w} 538_{w}	588_{w}	600_{av}		720^{v}_{w}	852_{w} 840_{w}	880_{av} 894_{av}	920_{av}	954_{w} 970^{av}_{wd}	1040^{av}_{wd}	1100_{av}		1162^{av}_{wd}	1236^{av}_{wd}	Si_3N_4 am α, Si, $SiO_x(x\leqslant 2)$
		60	400^{av}_{n} 445^{av}_{n}	480^{st}_{n} 500_{sh}	520_{w} 538_{w}	588_{w}	600_{w}	670_{w} 650_{w}	725_{w} $\begin{cases}794_{w}\\800\end{cases}$	856_{w} 842_{av}	880^{av}_{n} 894^{av}_{n}	925_{av}	970^{av}_{wd}	1040^{av}_{wd}	1100_{av}		1160^{av}_{wd}	1238^{av}_{wd}	Si_3N_4α, am., $SiO_x(x\leqslant 2)$, Traces of Si
		120	400^{st}_{n}	451^{av}_{n} 486^{st}_{n}	526_{w} 538_{av}	575_{av} 588_{w}	636_{w} 660_{w}	675_{w}	725_{w}	800_{w} 844^{st}_{n}	882^{av}_{n} 862_{w}	900^{w}_{n} 930_{w} 950_{w}	970_{w}	1034_{av} 1052_{av}	1100_{av} 1088_{av}		1175_{av}	1238^{av}_{wd}	Si_3N_4α $SiO_x(x\leqslant 2)$
		180	400^{st}_{n}	452^{st}_{n} 486^{st}_{n} 500_{sh}	530_{w} 544_{av}	565_{w} 588^{w}_{n}	620_{w} 630_{w}	656_{av} 678_{av}	730_{av}	846^{st}_{n}	862_{w} 888^{av}_{n}	900^{w}_{n} 930_{av}	970_{av}	1032_{av} 1050_{av}	1088_{av} 1106_{av}		1175_{av}	1238^{av}_{wd}	Si_3N_4α, β, $SiO_x(x\leqslant 2)$
		240	400^{st}_{n}	454^{st}_{n} 488^{st}_{n} 500_{sh}	527_{av} 538_{av}	570_{w} 594^{av}_{n}	640_{w}	670_{w} 677^{av}_{n}	730_{av}	802_{w} 846^{st}_{n}	862_{w} 888^{av}_{n}	900^{w}_{n} 930^{av}_{wd}	950_{w} 980^{av}_{wd}	1038^{st}_{wd}	1088^{st}_{wd} 1100_{w}		1175_{av}	1225^{av}_{wd}	Si_3N_4α, β, $SiO_x(x\leqslant 2)$
	1573	30	402^{st}_{n}	490^{st}_{n} 420_{w} 430_{w} 456^{st}_{n} 500_{sh}		596^{av}_{n} 575_{w}		670_{w} 680^{av}_{n}		800_{w} 850^{st}_{n}	864_{w} 888^{av}_{n}	900_{w} 938^{av}_{wd}	970^{av}_{wd}	1030^{st}_{wd}				Si_3N_4α, β
		60	400^{st}_{n}	480^{st}_{n} 430^{v}_{w} 456^{av}_{n} 500_{sh}		570_{w} 596^{av}_{n}	652_{w}	675^{av}_{n}		848^{st}_{n}	862_{w} 888^{av}_{n}	902_{w} 930^{av}_{wd}	950_{w} 970^{av}_{wd}	1030^{st}_{wd}				Si_3N_4α, β
		120	402^{st}_{n}	$488^{v.st}_{n}$ 425_{w} 456^{st}_{n} 500_{sh}	550_{av}	570_{w} 596_{w}	625_{w} 656_{av}	670^{av}_{n} 680^{av}_{n}	732_{w}	$850^{v.st}_{n}$	868_{w} 885^{av}_{n}	900_{w} 925^{av}_{wd}	975^{av}_{wd}	1038^{st}_{wd}					Si_3N_4, α, β
		180	400^{st}_{n}	488^{st}_{n} 430_{w} 454^{st}_{n} 500_{sh}		562_{w} 596_{w}	630_{w} 660_{av}	680^{av}_{n} 670^{av}_{n}	796_{w}	$850^{v.st}_{n}$	870_{w} 885^{av}_{n}	902_{w} 925^{av}_{wd}	975^{av}_{wd}	1050^{av}_{wd}					Si_3N_4, α, β
		480	400^{av}_{n}	490_{av} 454_{w}		$562_{v.w}$ 596_{w}	630_{w}	662_{w} 680_{w}		848_{av}	870_{w} 888_{w}	$902^{v.}_{w}$ 930^{av}_{wd}	975^{av}_{wd}	1030^{av}_{wd}					Si_3N_4, α, β
	1673	30	400^{st}_{n}	425_{w} 450_{av} 488^{st}_{n} 500_{sh}		590_{w}	652_{w}	676^{av}_{n} 680^{av}_{n}		844^{st}_{n} 856_{w}	882^{av}_{n}	900_{w} 930^{av}_{wd}	952_{w} 975^{w}_{wd}	1036^{st}_{wd}					Si_3N_4, α, β

12	Initial					615_w				980_w		1080^{av}_{wd}					Si, $SiO_x(x < 2)$
	973	20	440_w	470_{av}	506^{av}_{wd}	560^{av}_n	610^{av}_n		740_w	850_w	915_w	946_w	1062_w	1086_w	1150_{av}	1192_w	1212_w	Si_3N_4, am,
					510_w		600_w			890_w							1237_{av}	Si, $SiO_x(x < 2)$
	1473	20	440_w	455_w	494_{st}	562_w	610_w	675_w		854^{av}_n	880_w	988_w	1050_w	1088_w	1150_{av}	1196_w	1220_w	$Si_3N_{4\,am}$, α,
				470_w	510_w		600_w		760_w	870_w	906_w	945^{av}_{wd}					1235_{av}	$SiO_x(x \leqslant 2)$,
											915_w	962^{av}_{wd}						Traces of Si
		40	440_w	470_w	508_{av}	560_w	610_w		740^v_w	870_w	904_w	930^{av}_{wd}	1040^{av}_{wd}		1150_{av}	1196_{av}		Si_3N_4, α, am,
				455^{av}_n	494^{st}_n		600_w			850^{av}_n	890_{av}							$SiO_x(x \leqslant 2)$
		60	425_{av}	470_w	507_{av}		607_w	680_w			910_{st}	980^{st}_{wd}	1040_{st}					Si_3N_4, α, β

For the sample numbers see Table I.
*Si phases were identified using absorption bands referring to hypothetical Si_2O complexes.
The superscripts and subscripts are defined as follows:
st, strong;
n, narrow;
sh, shoulder;
w, weak;
v, very;
av, average; and
wd, wide.

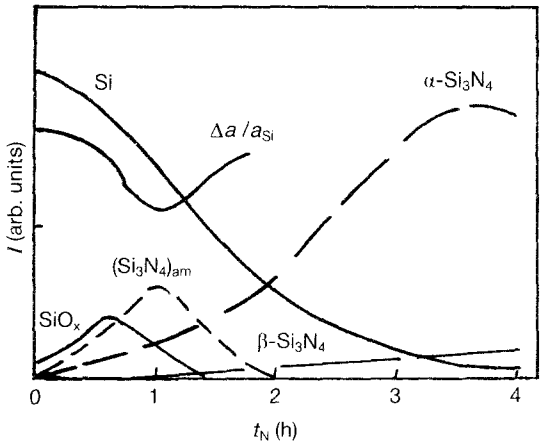

Figure 5 The scheme of the structural and phase transformations in the Si–N system.

With the increase in t_N, crystallization of the amorphous Si_3N_4 formed on the surface-defect silicon layers takes place, followed by the volume Si-particle-state nitriding. The mechanism of the latter is of particular importance.

Reaction gas–solid supposes nitrogen diffusion into particle volume. In the case under consideration, the nitrogen atoms' diffusion mobility into silicon ($D \sim 3.22 \times 10^{-8}$ cm^2 s^{-1} at 1683 K [1]) is obviously insufficient for nitriding in the whole particle volume. This is supported by the results for the nitriding of the etched samples. Thus, introduction of nitrogen atom into the volume of the unetched silicon particles follows another more complex mechanism – where the initial surface-defect structure acts as a catalyst of the diffusive (involving volumetric) processes. An increase in the silicon-lattice microstresses correlates with the nitriding silicon particles volumetric states at $t_N > 1$ h (see Fig. 3b). The principal cause for this is supposed to be specific formation of a silicon-nitride phase in the surface defect layer of silicon particles, initiating deformation distortions in the particle volume. On the basis of these concepts, we shall consider the possible role in deformation distortions played by microcracks which are stopped in the silicon-particle surface layer.

According to [9, 10] the region of the surface microcrack opening is filled with amorphous silicon. Since transformation into the amorphous state requires formation of about 6×10^{24} cm^{-1} of di- and tetravacancies in a crystal, the volume of the amorphous phase is larger than the crystalline analogue, and stress fields arise around microcracks. Heat treatment in a nitrogen medium promotes amorphous-silicon crystallization, that is, microcrack curing. On the other hand, such microcracks are diffusion passages of the volume nitriding (at microcrack depths). Silicon nitride formation in these passages prevents crack curing. Thus, the time the diffusion passages exist is prolonged. The content of Si_3N_4 formation is determined by the quantity of the reacted silicon. The nitride volume is 1.2 times that of the silicon volume forms from it, so nitride alone may be the source of the stresses resulting in the subsequent microcracking.

Such a chemico-mechanical effect should be self-activating, (the more nitride that is formed in the surface-microcrack mouth, the more cracks open; the

more cracks open, the greater is the sample volume nitriding, etc.

Furthermore, silicon primary particles may be completely fractured and new, finer, silicon-nitride particles, or their aggregates, may form on their base.

It should be noted that the differences in the magnitudes of the linear coefficients of thermal expansion ($\alpha_{Si} = 4.1 \times 10^{-6}\,deg^{-1}$, $\alpha_{Si_3N_4} = 2.75 \times 10^{-6}\,deg^{-1}$) may be the basic cause for Si_3N_4 surface layers spalling from the silicon "substrate" during transition from nitriding temperature to room temperature.

5. Conclusion

Low-temperature nitriding of silicon powders is determined by the silicon-particle defect structure formed during coarse-grained-powder comminuting. The defect structure of particles is described in terms of the two-layer model of the weakly distorted core and the surface layer with numerous microcracks filled with amorphous-silicon interlayers.

Volume nitriding of silicon powders is initiated by a chemico-mechanical effect, involving surface-nitride formation, which promotes mechanical stresses in a surface-silicon-particle layer, leading to opening (and nitriding) of the stopped micro cracks.

Acknowledgement

The authors wish to thank Dr N. F. Ostrovskaya and V. B. Zelyavsky for the X-ray analysis and the electron microphotography.

References

1. H. M. JENNINGS, *J. Mater. Sci.* **18** (1983) 951.
2. A. J. MOULSON, *ibid.* **14** (1979) 1017.
3. J. WEISS, *Ann. Rev. Mater. Sci.* **11** (1981) 381.
4. A. ATKINSON, A. J. MOULSON and E. W. ROBERTS, *J. Amer. Ceram. Soc.* **59** (1976) 285.
5. S. M. BOYER, D. SANG and A. J. MOULSON, "Nitrogen ceramics", edited by F. L. Riley (Noordhoff, Leyden, 1977) p. 297.
6. H. DERVISBEGOVIC and F. L. RILEY, *J. Mater. Sci.* **16** (1981) 1945.
7. H. M. JENNINGS and M. H. RICHMAN, *ibid.* **11** (1976) 2087.
8. NEMETALLICHESKIYE TUGOPLAVKIYE SOYEDINENIYA, T. YA. KOSOLAPOVA, T. V. ANDREEVA, T. S. BARTNITSKAYA *et al* M.: Metallurgiya (1985) 224 s. Non Metallic Refractory Systems.
9. M. V. VLASOVA and N. G. KAKAZEI, *Solid State Commun.* **47** (1983) 255.
10. S. I. GORBACHUK, N. G. KAKAZEI and V. N. MINAKOV *Dokl. AN SSSR*, **294** (1987) 1111.
11. T. S. BARTNITSKAYA, M. V. VLASOVA, V. B. ZELYAVSKY and N. G. KAKAZEI *Poroshkovaya Matallurgiya* **11** (1992) 1.
12. P. RAMA RAO and T. R. ANANTHARAMAN, *Z. Metallkde.* **54** (1963) 658.
13. D. HANEMAN, M. F. CHUNG and A. TALONI, *Phys. Rev.* **170** (1968) 719.
14. M. NAKAMURA, Y. MOCHIZUFI, K. USAMI, Y. ITOH and T. NOZAKI, *Solid State Commun.* **50** (1984) 1079.
15. A. S. BEREZHNOY, Kremny i Yego Binary Sistemi. K.: Izd-vo AN UkrSSR, (1958) 430 s. Silicon and its binary systems.

Received 16 June 1992
and accepted 9 September 1993